Acta Mech 208, 163–180 (2009)
DOI 10.1007/s00707-008-0133-4

**Masoud Asgari · Mehdi Akhlaghi · Seyed Mahmoud Hosseini**

# Dynamic analysis of two-dimensional functionally graded thick hollow cylinder with finite length under impact loading

Received: 12 April 2008 / Revised: 8 September 2008 / Published online: 24 January 2009


**Abstract** In this paper a thick hollow cylinder with finite length made of two-dimensional functionally graded material (2D-FGM) and subjected to impact internal pressure is considered. The axisymmetric conditions are assumed for the 2D-FG cylinder. The finite element method with graded material properties within each element is used to model the structure, and the Newmark direct integration method is implemented to solve the time dependent equations. The time histories of displacements, stresses and 2D wave propagation are investigated for various values of volume fraction exponents. Also the effects of mechanical properties distribution in radial and axial direction on the time responses of the FG cylinder as well as the stress distribution are studied and compared with a cylinder made of 1D-FGM. The achieved results show that using 2D-FGM leads to a more flexible design. To verify the presented method and data, the results are compared to published data.

## 1 Introduction

In recent years, the composition of several different materials is often used in structural components in order to optimize the responses of structures subjected to thermal and mechanical loads. Functionally graded materials (FGMs) are suitable to achieve this purpose. The mechanical properties of FGMs vary continuously between several different materials. This idea was used for the first time by Japanese researchers [1], leads to the concept of FGMs. Most of researches in this area are concerned with the thermo-elastic and residual stress analysis. In many applications of these materials the dynamic behavior and wave propagation characteristics are of great importance in addition to thermal and residual stress considerations. One-dimensional stress wave propagation was considered by Liu et al. [2], Chui et al. [3] and Bruck [4]. The response of a functionally graded metal-ceramic plate under impulsive loading was discussed by Li et al. [5]. Also Han et al. [6] studied the response of FGM plates under impact loads in three dimensions numerically. Berezovski et al. [7] analyzed the numerical simulation of 2D wave propagation in FGMs by two distinct models as multi layered and randomly embedded particles with prescribed volume fraction. Barta and Love [8] used FEM to analyze transient plane strain deformation of an FG elastic body. Zhang and Batra [9] used a meshless method, namely the modified smoothed particle hydrodynamics, to study an elasto-dynamic problem and propagation of an elastic wave in FGM. Shakeri et al. [10] presented the vibration and radial wave propagation velocity in a functionally graded

M. Asgari · M. Akhlaghi (✉)
Mechanical Engineering Department, Amirkabir University of Technology, P.O. Box 15875-4413,
Hafez Avenue, Tehran, Iran
E-mail: makhlagi@aut.ac.ir
Tel.: +98-21-64543409
Fax: +98-21-66419736

S. M. Hosseini
Mechanical Engineering Department, Khorasan Research Institute of Sciences and Food Technology,
P.O. Box 91735-139, Mashhad, Iran

thick hollow cylinder under dynamic loading by dividing the cylinder into many homogeneous sub-cylinders. Hosseini et al. [11] studied the dynamic responses and natural frequencies of a functionally graded cylinder under internal pressure. In most of the cases mentioned the variation of volume fraction and properties of the FGMs are 1D and properties vary continuously from one surface to the other with a prescribed function. But conventional FGM may also not be so effective in some design problems since all outer or inner surfaces will have the same composition distribution while in advanced machine elements temperature and load distribution may change in two or three directions [12]. Therefore, if the FGM has 2D dependent material properties more effective material resistance can be obtained. Based on this fact, a 2D-FGM whose material properties are bi-directionally dependent is introduced. Recently a few authors have investigated 2D-FGM. Dhaliwal and Singh [13] solved the equations of equilibrium for a non-homogeneous elastic solid under shearing forces. The modulus of rigidity of their considered material varied exponentially in lateral and vertical direction. Clement et al. [14] considered the solution of anti plane deformation in homogenous elasticity when the shear modulus varied with two Cartesian coordinates. Aboudi et al. [15] studied thermo-elastic/plastic theory for the response of materials functionally graded in two directions. Cho and Ha [16] optimized the volume fraction distributions of 2D-FGM for relaxing the effective thermal stresses. Hedia et al. [17] modeled the backing shell of the cemented acetabular cup with 2D-FGM and compared its performance in the reduction of stress against 1-D FGM cup.

There are numerous numerical methods to model the variation of material properties in FGMs. Conventional finite element formulations use a single material property for each element such that the property field is constant within an individual element. But using this method for wave propagation and dynamic problems leads to significant discontinuities and inaccuracies [18]. These inaccuracies will be more significant in 2D-FGM cases. Banks et al. [19] investigated the effects of using different FEM approximations on the stress wave propagation through the graded materials. Scheidler and Gazonas [20] considered wave propagation in an elastic medium with a quadratic impedance variation through the thickness, subjected to both step and impact loading. Sentare and Lambros [21] and Kim and Paulino [22] showed that graded finite elements can improve accuracy without increasing the number of degrees of freedom and decreasing the size of elements.

Analyses of dynamic loading and wave propagation in thick hollow cylinders with finite length made of 2D-FGMs were not seen in the previous literatures. In this paper, a thick hollow cylinder with finite length made of 2D-FGM is considered. The material properties of this cylinder are varied in the radial and axial directions with power law functions. The response of the structure under dynamic internal pressure, introduced by an impact function is investigated. The time history of displacements and stresses, 2D distribution of stresses in the cylinder and 2D stress wave propagation are studied for various kinds of mechanical properties variations in 2D-FGM cylinders. The cylinder is considered in axisymmetric conditions. The effects of 2D mechanical properties distribution across the thickness and length of the cylinder on the time responses and other parameters such as stress distributions and stress wave propagation are obtained, and some of them are compared to data from a 1D FG cylinder.

## 2 Problem formulation

In this Section volume fraction distributions in the two radial and axial directions are introduced. The governing equations of motion in axisymmetric cylindrical coordinates are obtained, and graded finite element is used for modeling the non-homogeneity of the material.

### 2.1 Volume fraction and material distribution in 2D-FGM cylinder

In the conventional 1D functionally graded cylinder, the cylinder's material is graded in the radial direction. The cylinder is made of a combined metal-ceramic material for which the mixing ratio is varied continuously in the $r$-direction from pure ceramic in the inner surface to pure metal in the outer surface or vice versa. In such cases the volume fraction variation of the metal is proposed as [10]

$$V_{\mathrm{m}}(r) = \left(\frac{r - r_{\mathrm{i}}}{r_{\mathrm{o}} - r_{\mathrm{i}}}\right)^{n}, \tag{1}$$

where $r_{\mathrm{i}}$ and $r_{\mathrm{o}}$ denote the inner and outer radii of the hollow cylinder and $n$ is a non-negative constant.

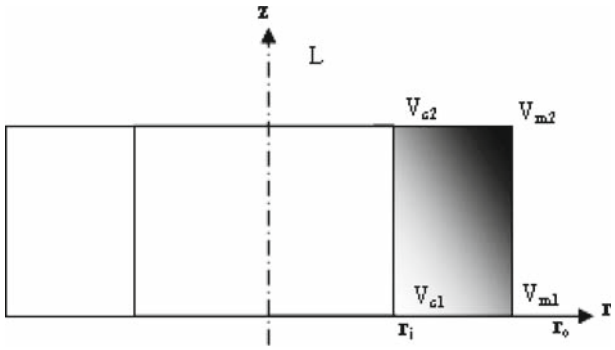


**Fig. 1** Axisymmetric cylinder with two-dimensional material distribution

Using the rule of mixtures, the distribution of the material properties is given by

$$P = (P_{\mathrm{m}} - P_{\mathrm{c}}) \left( \frac{r - r_{\mathrm{i}}}{r_{\mathrm{o}} - r_{\mathrm{i}}} \right)^{n} + P_{\mathrm{c}}, \tag{2}$$

where $P$ is the material property such as mass density and modulus of elasticity. And $m$ and $c$ subscripts stand for metal and ceramic.

Two-dimensional FGMs are usually made by continuous gradation of three or four distinct material phases where one or two of them are ceramics and the others are metal alloy phases, and the volume fractions of the constituents vary in a predetermined composition profile. Now consider the volume fractions of 2D-FGM at any arbitrary point in the 2D-FG axisymmetric cylinder shown in Fig. 1. In the present cylinder the inner surface is made of two distinct ceramics and the outer surface of two metals. c1, c2, m1 and m2 denote first ceramic, second ceramic, first metal and second metal, respectively. Also $r_{\mathrm{i}}, r_{\mathrm{o}}$ and $L$ are internal radius, external radius and length of cylinder, respectively.

The volume fraction of the first ceramic material is changed from 100% at the lower surface to zero at the upper surface. And also this volume fraction changes continuously from inner surface to the outer surface. In other words the volume fraction varies in the radial and axial directions with predetermined continuous functions. Volume fractions of the other materials change similar to the mentioned one in two directions. The volume fraction distribution function of each material can be explained as

$$V_{\mathrm{c1}} = \left[ 1 - \left( \frac{r - r_{\mathrm{i}}}{r_{\mathrm{o}} - r_{\mathrm{i}}} \right)^{n_r} \right] \left[ 1 - \left( \frac{z}{L} \right)^{n_z} \right], \tag{3}$$

$$V_{\mathrm{c2}} = \left[ 1 - \left( \frac{r - r_{\mathrm{i}}}{r_{\mathrm{o}} - r_{\mathrm{i}}} \right)^{n_r} \right] \left[ \left( \frac{Z}{L} \right)^{n_z} \right], \tag{4}$$

$$V_{\mathrm{m1}} = \left( \frac{r - r_{\mathrm{i}}}{r_{\mathrm{o}} - r_{\mathrm{i}}} \right)^{n_r} \left[ 1 - \left( \frac{Z}{L} \right)^{n_z} \right], \tag{5}$$

$$V_{\mathrm{m2}} = \left( \frac{r - r_{\mathrm{i}}}{r_{\mathrm{o}} - r_{\mathrm{i}}} \right)^{n_r} \left( \frac{Z}{L} \right)^{n_z}, \tag{6}$$

where subscripts c1, c2, m1 and m2 denote first ceramic, second ceramic, first metal and second metal, respectively. Also $n_r$ and $n_z$ are non-zero parameters that represent the basic constituent distributions in $r$- and $z$-directions. From proposed volume fraction functions, the volume fractions of the basic materials on each boundary surface are

$$\begin{array}{llllll}
\text{at} & r = r_{\mathrm{i}}, & z = 0 \Rightarrow V_{\mathrm{c1}} = 1, & V_{\mathrm{c2}} = 0, & V_{\mathrm{m1}} = 0, & V_{m2} = 0, \\
\text{at} & r = r_{\mathrm{o}}, & z = 0 \Rightarrow V_{\mathrm{c1}} = 0, & V_{\mathrm{c2}} = 0, & V_{\mathrm{m1}} = 1, & V_{m2} = 0, \\
\text{at} & r = r_{\mathrm{i}}, & z = L \Rightarrow V_{\mathrm{c1}} = 0, & V_{\mathrm{c2}} = 1, & V_{\mathrm{m1}} = 0, & V_{m2} = 0, \\
\text{at} & r = r_{\mathrm{o}}, & z = L \Rightarrow V_{\mathrm{c1}} = 0, & V_{\mathrm{c2}} = 0, & V_{\mathrm{m1}} = 0, & V_{m2} = 1.
\end{array}$$

For instance, the volume fraction distributions of two basic materials for the typical values of $n_r = 2$ and $n_z = 3$ are shown in Figs. 2 and 3. In this case $r_{\mathrm{i}} = 1\,\mathrm{m}$, $r_{\mathrm{o}} = 1.5\,\mathrm{m}$, $L = 1\,\mathrm{m}$.

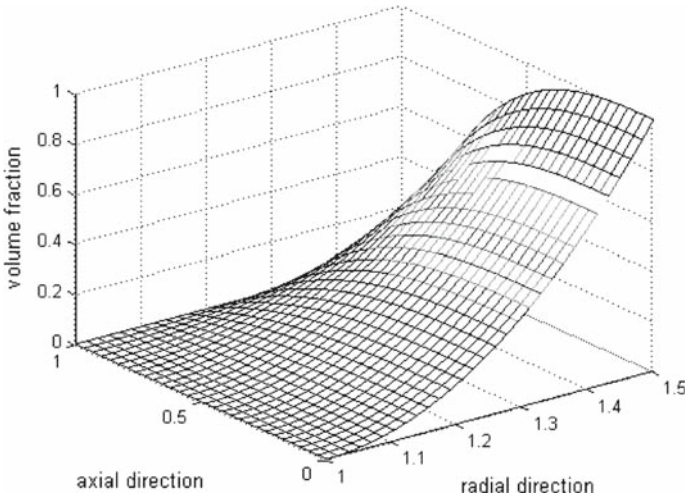


**Fig. 2** Volume fraction distribution of m1

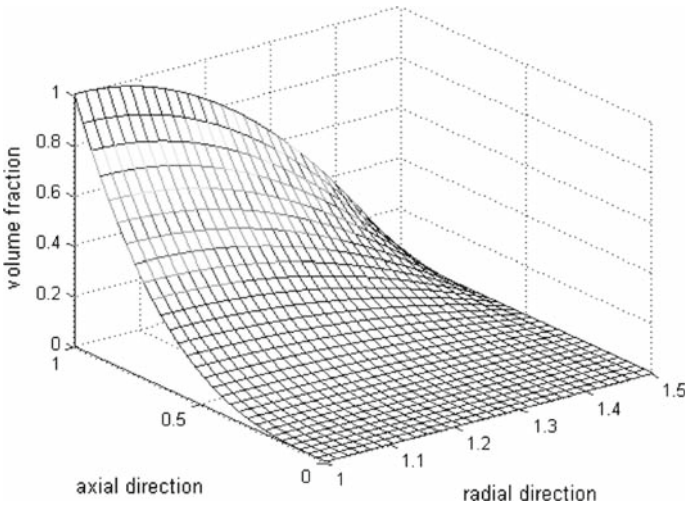


**Fig. 3** Volume fraction distribution of c2

**Table 1** Basic constituents of the 2D-FGM cylinder

| Constituents | Material | $E(GPa)$ | $\rho$ (kg/m$^3$) |
|---|---|---|---|
| m1 | Ti6Al4V | 115 | 4,515 |
| m2 | Al 1,100 | 69 | 2,715 |
| c1 | SiC | 440 | 3,210 |
| c2 | $Al_2O_3$ | 300 | 3,470 |

The material properties at each point can be obtained by using the linear rule of mixtures in which a material property, $P$, at an arbitrary point, $(r, z)$ in the 2D-FGM cylinder is determined by linear combination of volume fractions and material properties of basic materials as

$$P = P_{c1}V_{c1} + P_{c2}V_{c2} + P_{m1}V_{m1} + P_{m2}V_{m2}. \tag{7}$$

The basic constituents of the 2D-FGM cylinder are presented in Table 1.

The distribution of one typical material property, mass density, through the cylinder is shown in Fig. 4.

It should be noted that Poisson's ratio is assumed to be constant through the body. This assumption is reasonable because of small differences between the Poisson's ratios of the basic materials.

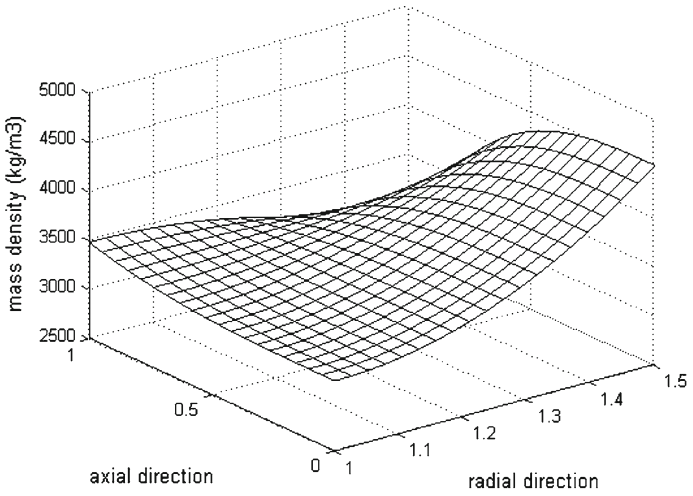


**Fig. 4** Distribution of mass density through the cylinder

## 2.2 Governing equations

Consider a 2D-FG thick hollow cylinder of internal radius $r_i$, external radius $r_o$ and finite length $L$. Because of the axisymmetric geometry and loading, coordinates $r$ and $z$ are used in the analysis. Neglecting body forces, the equations of motion in axisymmetric cylindrical coordinates are obtained as

$$\frac{\partial \sigma_{rr}}{\partial r} + \frac{\sigma_{rr} - \sigma_{\theta\theta}}{r} + \frac{\partial \tau_{rz}}{\partial z} = \rho(r,z)\frac{\partial^2 u}{\partial t^2}, \tag{8}$$

$$\frac{\partial \tau_{rz}}{\partial r} + \frac{\partial \sigma_{zz}}{\partial z} + \frac{\tau_{rz}}{r} = \rho(r,z)\frac{\partial^2 w}{\partial t^2}, \tag{9}$$

where $u$ and $w$ are radial and axial components of displacement, respectively, and $\rho(r,z)$ is the mass density that depends on $r$ and $z$ coordinates. The constitutive equations for FGM are written as

$$\{\sigma_{ij}\} = [D_{ij}]\{\varepsilon_{ij}\}, \tag{10}$$

where the stress and strain components and the coefficients of elasticity are

$$\{\sigma_{ij}\} = \begin{bmatrix} \sigma_{rr} & \sigma_{\theta\theta} & \sigma_{zz} & \tau_{rz} \end{bmatrix}, \tag{11}$$

$$\{\varepsilon_{ij}\} = \begin{bmatrix} \varepsilon_{rr} & \varepsilon_{\theta\theta} & \varepsilon_{zz} & \varepsilon_{rz} \end{bmatrix}, \tag{12}$$

$$[D] = \frac{E(r,z)}{(1+\nu)+(1-2\nu)} \begin{bmatrix} 1-\nu & \nu & \nu & 0 \\ \nu & 1-\nu & \nu & 0 \\ \nu & \nu & 1-\nu & 0 \\ 0 & 0 & 0 & \frac{1-2\nu}{2} \end{bmatrix}, \tag{13}$$

where $\nu$ denotes the Poisson's ratio and $E(r,z)$ is Young's modulus that depends on $r$ and $z$ coordinates. The strain-displacement equations are [23]

$$\varepsilon_r = \frac{\partial u}{\partial r}, \tag{14.1}$$

$$\varepsilon_\theta = \frac{u}{r}, \tag{14.2}$$

$$\varepsilon_z = \frac{\partial w}{\partial z}, \tag{14.3}$$

$$\gamma_{rz} = \frac{\partial u}{\partial z} + \frac{\partial w}{\partial r}. \tag{14.4}$$

The cylinder is clamped on its two end edges. It is subjected to axisymetric internal pressure that varies with time. Thus, the mechanical boundary conditions on upper and lower surfaces are assumed as

$$u(r,0) = u(r,L) = w(r,0) = w(r,L) = 0 \tag{15}$$

and also on the inner and outer surfaces are

$$\sigma_{rr}(r_\mathrm{i},z) = P_\mathrm{i}(z,t), \tag{16}$$

$$\sigma_{rr}(r_\mathrm{o},z) = \tau_{rz}(r_\mathrm{i},z) = \tau_{rz}(r_\mathrm{o},z) = 0. \tag{17}$$

It is notable that the present solution method can be used for any arbitrary function of time as the load function. The variation of internal pressure with time and its distribution along the axial direction will be described later.

### 2.3 Graded finite element modeling

In order to solve the governing equations the finite element method with graded element properties is used. For this purpose the Ritz's variational formulation is considered. In conventional finite element formulations a predetermined set of material properties is used for each element such that the property field is constant within an individual element. For modeling a continuously non-homogeneous material, the material property function must be discretized according to the size of element's mesh. This approximation can provide significant discontinuities. These artificial discontinuities especially in dynamic and wave propagation problems can cause an enormous error in the results [18]. On the other hand, using a graded finite element in which the material property field is graded continuously through the elements, the accuracy can be improved without refining the mesh size [21,22]. In addition, the variation of material properties in two directions such as the present problem makes this effect more considerable. Based on these facts the graded finite element is strongly preferable for modeling of the present problem.

Hamilton's principle for the present problem is

$$\int_{t_1}^{t_2} \delta(U - T - W)\mathrm{d}t = 0, \tag{18}$$

where $U$, $T$ and $W$ are potential energy, kinetic energy and virtual work done by surface tractions, respectively. These functions and their variations are

$$T = 1/2 \int_V \rho \dot{u}_i \dot{u}_i \mathrm{d}V, \tag{19.1}$$

$$\delta T = \int_V \rho \ddot{u}_i \delta V, \tag{19.2}$$

$$U = \int_V \sigma_{ij}\varepsilon_{ij}\mathrm{d}V, \tag{20.1}$$

$$\delta U = \int_V \sigma_{ij}\delta\varepsilon_{ij}\mathrm{d}V, \tag{20.2}$$

$$W = \int_A p_i u_i \mathrm{d}A, \tag{21.1}$$

$$\delta W = \int_A p_i \delta u_i \mathrm{d}A, \tag{21.2}$$

where $A$ and $V$ denote the area and volume of the domain under consideration and $p_i$ is the component of surface tractions.

Substituting Eqs. (19)–(21) in Hamilton's principle and applying side conditions, $\delta u_i(t_1) = \delta u_i(t_2) = 0$, and by part integration we have

$$\int_V \sigma_{ij}\delta\varepsilon_{ij}\mathrm{d}V + \int_V \rho\ddot{u}_i\delta u_i\mathrm{d}V = \int_A p_i\delta u_i\mathrm{d}A. \tag{22}$$

The strain-displacement relations can be written as

$$\{\varepsilon\} = [L]\{u\}, \tag{23}$$

where

$$\{\varepsilon\} = \begin{Bmatrix} \varepsilon_{rr} \\ \varepsilon_{\theta\theta} \\ \varepsilon_{\theta z} \\ \varepsilon_{rz} \end{Bmatrix}, \tag{24.1}$$

$$[L] = \begin{bmatrix} \partial/\partial r & 0 \\ 1/r & 0 \\ 0 & \partial/\partial z \\ \frac{1}{2}\,\partial/\partial z & \frac{1}{2}\partial/\partial r \end{bmatrix}, \tag{24.2}$$

$$\{u\} = \begin{Bmatrix} u \\ w \end{Bmatrix}. \tag{24.3}$$

An axisymmetric ring element with triangular cross-section is used to discrete the domain. By taking the nodal values of $u$ and $w$ as the degrees of freedom a linear displacement model can be assumed as [23]

$$\begin{Bmatrix} u(t) \\ w(t) \end{Bmatrix}^e = [N]\left\{Q^e(t)\right\}, \tag{25}$$

where $[N]$ is the matrix of linear interpolation functions and $\{Q^e(t)\}$ is the nodal displacement vector of the element. Components of them are given in the Appendix.

Using Eqs. (24) and (25) we can write

$$\{\varepsilon\} = [B]\left\{Q^e\right\}, \tag{26}$$

where

$$[B] = [L][N], \tag{27}$$

where the components of matrix $[B]$ are given in the Appendix.

Applying Hamilton's principle for each element and substituting Eqs. (10), (25) and (26), it can be achieved

$$\begin{aligned} &\delta\left\{Q^e\right\}^{\mathrm{T}}\left[\int_{V^e}[B]^{\mathrm{T}}[D][B]\mathrm{d}V\right]\left\{Q^e\right\} + \delta\left\{Q^e\right\}^{\mathrm{T}}\left[\int_{V^e}\rho[N]^{\mathrm{T}}[N]\mathrm{d}V\right]\left\{\ddot{Q}^e\right\} \\ &= \delta\left\{Q^e\right\}^{\mathrm{T}}\left[\int_{S^e}\rho[N]^{\mathrm{T}}\{P\}\mathrm{d}s\right], \end{aligned} \tag{28}$$

where $V^e$, $S^e$ and $\{P\}$ are volume of element, area under pressure and vector of surface tractions, respectively.

In a graded finite element, the interpolation function for the displacements within the elements and the strain-displacement relations are the same as for standard conventional finite element as for explained in Eqs. (24) and (25). In this way the constitutive relation is

$$\{\sigma(r,z)\} = [D(r,z)]\{\varepsilon(r,z)\}, \tag{29}$$

where the components of $[D(r, z)]$ could be explicit functions describing the actual material property gradient in which $E(r, z)$ is determined at each point through the element using the distribution function of this property based on the rule of mixtures as

$$E(r, z) = E_{c1} V_{c1}(r, z) + E_{c2} V_{c2}(r, z) + E_{m1} V_{m1}(r, z) + E_{m2} V_{m2}(r, z). \tag{30}$$

And also, the mass density $\rho(r, z)$ is in general a function of position as well as of the mechanical properties. Therefore in the graded finite element the mass density distribution should be assigned to the element formulation same as the stiffness property as

$$\rho(r, z) = \rho_{c1} V_{c1}(r, z) + \rho_{c2} V_{c2}(r, z) + \rho_{m1} V_{m1}(r, z) + \rho_{m2} V_{m2}(r, z). \tag{31}$$

Using Eqs. (29)–(31) and substituting them to Eq. (28) we have

$$[M]^e \{\ddot{Q}\} + [K]^e \{Q\} = \{F\}^e, \tag{32}$$

where the characteristic matrices are given as

$$[K]^e = \int_V [B(r, z)]^{\mathrm{T}} [D(r, z)] [B(r, z)] \, \mathrm{d}V, \tag{33}$$

$$[M]^e = \int_V [N(r, z)]^{\mathrm{T}} [N(r, z)] \, \rho(r, z) \mathrm{d}V, \tag{34}$$

$$\{F\}^e = \int_{s^c} [N]^{\mathrm{T}} \{P\} \, \mathrm{d}s. \tag{35}$$

For finding the components of characteristic matrices the integral must be taken over the elements' volume. Also neglecting body forces and initial strains (caused by temperature) the load vector due to surface tractions can be evaluated by integration over surfaces under pressure. As $[D(r, z)]$ and $\rho(r, z)$ are not constant, these matrices are evaluated by numerical integration for each element.

Now by assembling the element matrices, the global matrix equation for the structure can be obtained as

$$[M] \{\ddot{Q}\} + [K] \{Q\} = \{F\}. \tag{36}$$

Once the finite element equations are established, the Newmark [23] direct integration method with suitable time step is used to solve the equations.

## 3 Implementation and validation

To verify the present work, consider a finite length functionally graded thick hollow cylinder with simply supported end conditions. The material distribution is assumed to be 1D and it varies in radial direction from ceramic (alumina) at the inner surface to metal (aluminum) at the outer surface with a power law function with the exponent $n = 2$. The load is assumed to be a hydrostatic internal pressure. This problem has a semi-analytical series solution. The governing equations can be solved using the common multi-layer approach. In this way the FGM cylinder is divided to $m$ sub-cylinders and each layer is assumed to be homogeneous.

The geometrical parameters are length of $L = 1$ m, inner radius of $r_i = 1$ m and outer radius of $r_o = 1.5$ m.

The internal pressure is

$$P_i(z) = 10^6 \sin\left(\frac{\pi z}{L}\right). \tag{37}$$

The boundary conditions on the inner and outer surfaces of the cylinder are

$$\sigma_r^1(r_i, z) = P_i(z), \tag{38.1}$$

$$\tau_{rz}^1(r_i, z) = 0, \tag{38.2}$$

$$\sigma_r^m(r_o, z) = \tau_{rz}^m(r_o, z) = 0, \tag{38.3}$$

where the superscripts 1 and $m$ denote the inner and outer layers.

And on the upper and the lower ends they are assumed as

$$u^i(r,0) = \sigma_z^i(r,0) = \tau_{rz}^i(r,0) = 0, \quad i = 1,2,\ldots,m, \tag{39.1}$$

$$u^i(r,L) = 0, \sigma_z^i(r,L) = \tau_{rz}^i(r,L) = 0, \quad i = 1,2,\ldots,m, \tag{39.2}$$

where superscript $i$ denotes the number of layers.

The continuity conditions to be enforced at any interface between two layers are written as

$$\begin{aligned} &\sigma_r^{i-1}(r_\mathrm{i},z) = \sigma^i(r_\mathrm{i},z), \\ &\tau_{rz}^{i-1}(r_\mathrm{i},z) = \tau_{rz}^i(r_\mathrm{i},z), \quad i = 2,3,\ldots,m-1. \end{aligned} \tag{40}$$

The solution of the governing equations for each layer can be expressed as the following sinusoidal series solution that satisfies the boundary conditions [24]:

$$u(r,z) = \sum_{n=1}^{\infty} \varphi_n(r) \sin\left(\frac{n\pi z}{L}\right), \tag{41.1}$$

$$w(r,z) = \sum_{n=1}^{\infty} \psi_n(r) \sin\left(\frac{n\pi z}{L}\right). \tag{41.2}$$

Substituting the above series in the governing equations and applying boundary conditions and continuity conditions the unknown coefficients, $\varphi_n(r)$ and $\psi_n(r)$, can be found.

On the other hand for solving the mentioned problem by the graded finite element method developed here we suppose that the material properties vary in the radial direction only and the volume fraction exponents and property coefficients are taken as

$$n_z = 0, \quad n_r = 2, \quad P_{\mathrm{c}1} = P_{\mathrm{c}2} = P_\mathrm{c}, \quad P_{\mathrm{m}1} = P_{\mathrm{m}2} = P_\mathrm{m}.$$

$P_\mathrm{c}$ are material properties of the inner surface which is considered ceramic (alumina), and $P_\mathrm{m}$ are material properties of the outer surface which is metal (aluminum).The modulus of elasticity and the mass density at the inner radius are $E_\mathrm{c} = 380\,\mathrm{Gpa}$, $\rho_\mathrm{c} = 3{,}800\,\mathrm{kg/m^3}$. And those of the outer radius are $E_\mathrm{m} = 70\,\mathrm{Gpa}$, $\rho_\mathrm{m} = 2{,}707\,\mathrm{kg/m^3}$.

The internal pressure exerts a transient function as

$$P_i(z,t) = 10^6(1 - \mathrm{e}^{-ct}) \sin\left(\frac{\pi z}{L}\right),$$

where $c = 10^6 1/\mathrm{s}$.

The dynamic responses of the FGM cylinder subjected to internal pressure given by Eq. (41) in a long time can be considered as the steady state response of a cylinder under static load. The boundary conditions are assumed to be simply supported. The results for a long time (after $t = 1{,}000$ s) are compared with the achieved data in static analysis of a finite length cylinder which were solved by multi-layer approach. The comparison of the results in Fig. 5 shows good agreement between them.

The presented method in this paper can be verified using data of 1D FG cylinder under dynamic load which were previously published. To achieve this purpose, the distribution of mechanical properties is considered 1D and across the thickness of the FG cylinder. The boundary conditions on the inner and outer radii are assumed the same as [11] and the top and end of it are simply supported. The cylinder is assumed to be too long and the displacement response of a middle point across the length of the cylinder is considered. The obtained results are then compared with the published data. Figure 6 shows good agreement between the results at all points.

## 4 Numerical results and discussion

A thick hollow cylinder of inner radius $r_\mathrm{i} = 1\,\mathrm{m}$, outer radius $r_\mathrm{o} = 1.5\,\mathrm{m}$ and length $L = 1\,\mathrm{m}$ is considered for analysis. A functionally graded cylinder with 2D gradation of the distribution profile has been investigated as well as the case where the axial power law exponent is assumed zero, $n_z = 0$, the results of 1D gradation of the material distribution can be obtained in the hollow cylinder and the FGM will be 1D. The basic materials are as explained in the previous Section. Constituent materials are two distinct ceramics and two distinct metals

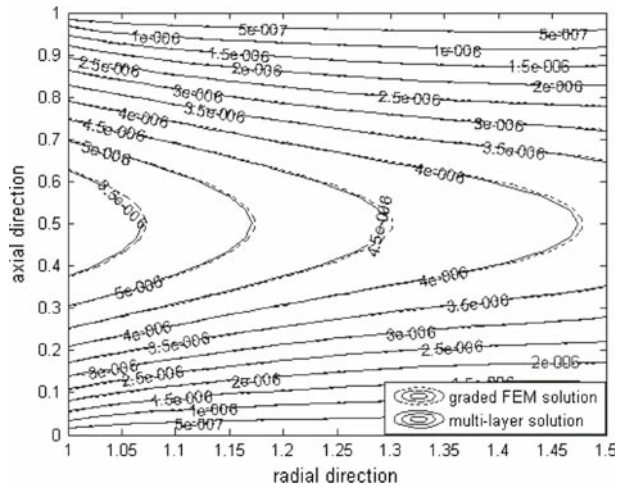


**Fig. 5** Radial displacement distribution through the cylinder for long time compared with static solution

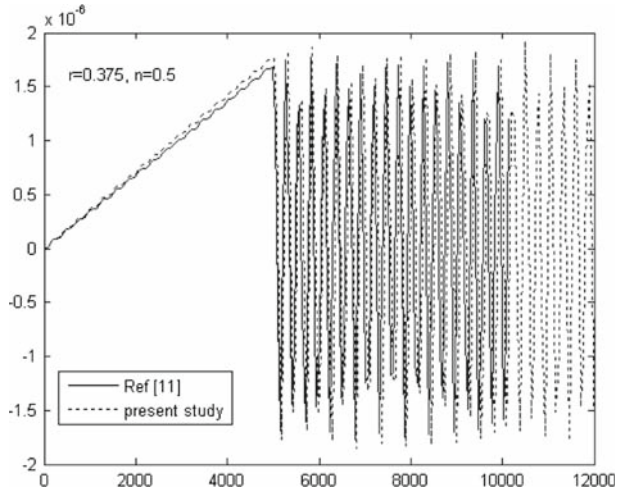


**Fig. 6** Time history of radial displacement at the middle point of the cylinder compared with infinite cylinder

described in Table 1. Volume fractions of the materials are distributed according to Eqs. (3)–(6). Dynamic responses of the cylinder for some different powers of material composition profile $n_r$ and $n_z$ are presented and compared. The internal pressure varies with time as an impact function, and it is distributed sinusoidally in the $z$-direction, which is expressed as

$$P_i(z,t) = \begin{cases} P_0 \mathrm{e}^{-a(t-t_0)^2} \sin\left(\frac{3\pi z}{L}\right) & \text{for } z \le L/3, \\ 0 & \text{for } z \ge L/3, \end{cases} \tag{42}$$

where $P_o$ is the maximum amplitude of the pressure, $a$ and $t_0$ are constants that determine the occurrence time and duration of the load. In the present study the internal pressure is distributed sinusoidally in the z-direction and also it is exerted on a finite portion of the cylinder length as shown in the Fig. 7.

Insertion of pressure in this manner instead of the case where the whole length is under pressure has two reasons. By this way the propagation of the stress wave in two directions is more observable and also in some real applications such as a combustion engine the load is exerted in a same manner. Variation of the internal pressure with time as an impact load is shown in Fig. 8 for typical values of $P_0 = 10^6$ Pa, $a = 4 \times 10^8$, $t_0 = 15 \times 10^{-5}$ s.

A cylinder with variation of volume fraction and material properties in two directions is considered. The basic materials are as explained in the previous Section. If the axial power law exponent is zero, $n_z = 0$, the material properties will vary in radial direction only and the FGM will be 1D.

Figure 9 shows the time history of radial displacement of a specified point in the 2D FGM cylinder. Power law exponents of the material distribution profiles in radial and axial directions are the same, $n_r = n_z = n$,

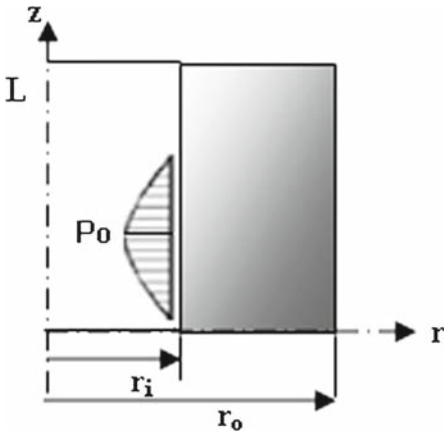


**Fig. 7** Variation of internal pressure along the axial direction

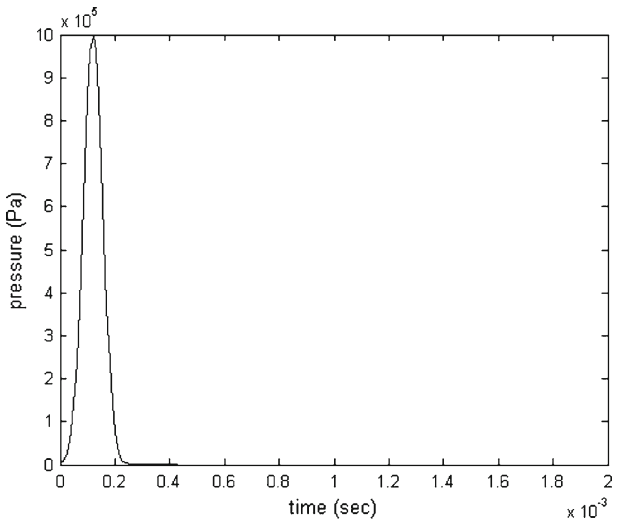


**Fig. 8** Variation of internal pressure with time

in the 2D cases. It can be seen that the maximum value of the amplitude is increased when the value of "$n$" is decreased. It means that the dynamic behavior of the cylinder tends towards the behavior of the cylinder which is made of full second metal (m2).

Time histories of radial, hoop and axial stresses for different power law exponents in the 2D and 1D FGM cylinder are denoted in Figs. 10, 11 and 12. It is evident from these figures that both of amplitude and time delay of the response are strongly affected by the material distribution power $n$. The hoop stress diagram is in a periodic form and it is concluded that the frequency of variation in the time domain (period time) is increased when the value of "$n$" is decreased. The maximum value of axial stress varies with "$n$" and the maximum value of axial stress for small value of "$n$" is bigger than values for big values of "$n$" as it is illustrated in Fig. 12. The maximum magnitude of axial stress is larger than that of radial stress, and smaller than that of hoop stress.

In order to have a more clear observation, the distributions of radial and hoop stresses through the thickness of the cylinder at a specific time are illustrated in Figs. 13 and 14 for different values of $n_r$ and $n_z$. These figures denote that maximum stress and stress distribution can be controlled by material distribution, and this is one of the best benefits of the presented method to determine the optimal design of a 2D-FGM cylinder which can be used by other researchers in the future.

The phenomenon of stress wave front is observed due to 2D-FGM modeling, and the governing equations are solved by hybrid finite element and finite difference numerical methods. The wave propagation scheme in a 2D-FGM cylinder can be observed in Fig. 15a–d. In these figures the radial stress distributions through the

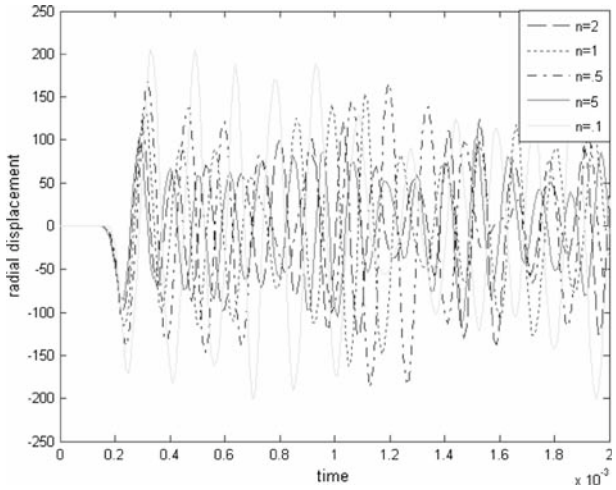


**Fig. 9** Time history of radial displacement at $r = 1.75$, $z = 0.5$ for $n_r = n_z = n$

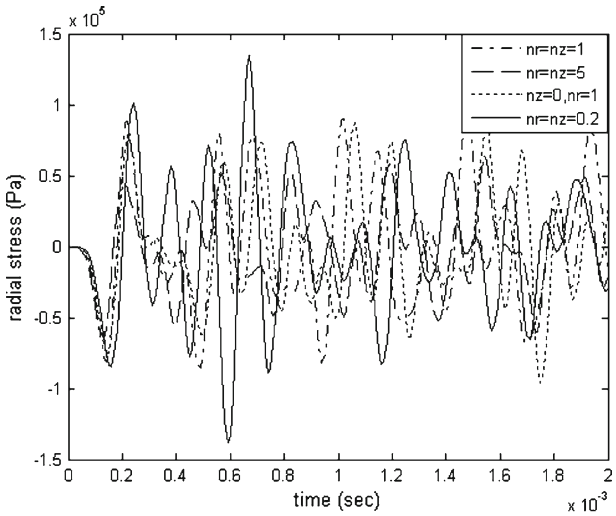


**Fig. 10** Time history of radial stress at $r = 1.75$, $z = 0.5$ for different $n_r$ and $n_z$

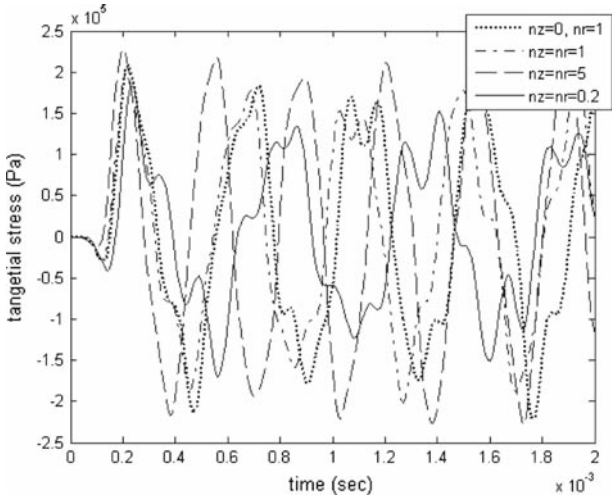


**Fig. 11** Time history of hoop stress at $r = 1.75$, $z = 0.5$ for different $n_r$ and $n_z$

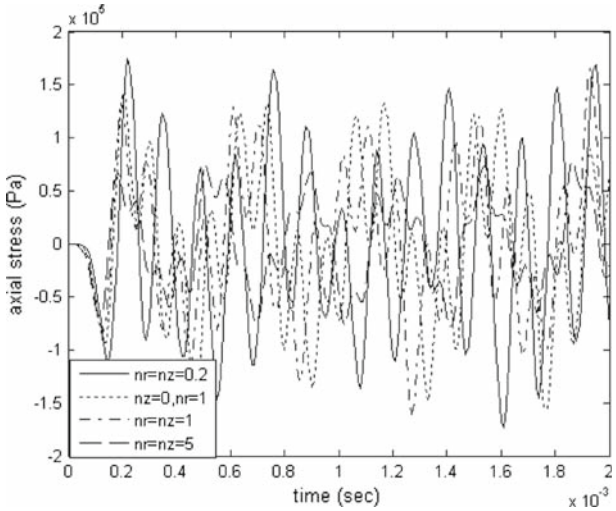


**Fig. 12** Time history of axial stress a at $r = 1.75$, $z = 0.5$ for different $n_r$ and $n_z$

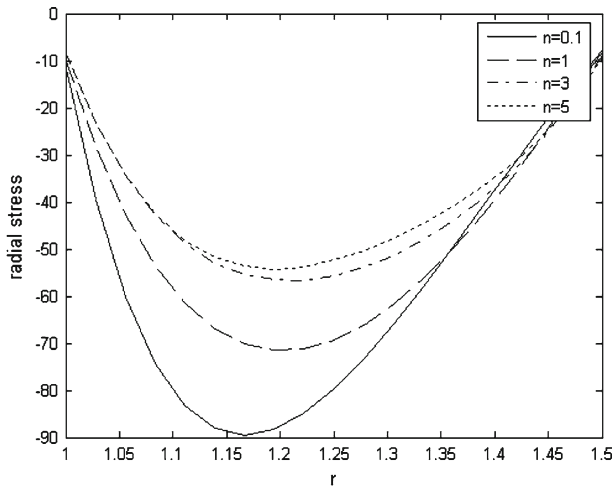


**Fig. 13** Distribution of radial stress through the thickness of cylinder at $t = 4 \times 10^{-4}$ s $n_r = n_z = n$

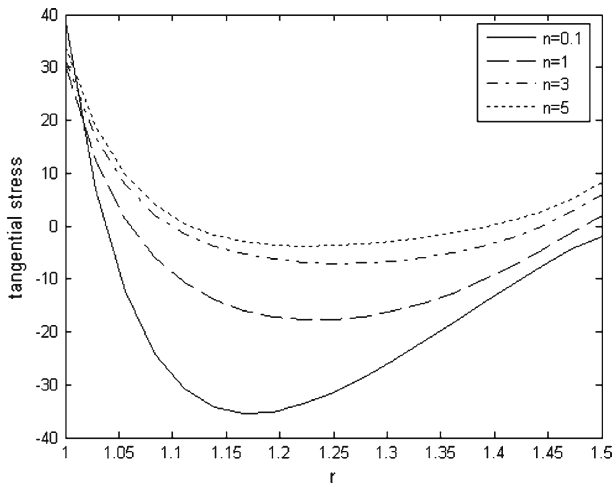


**Fig. 14** Distribution of hoop stress through the thickness of cylinder at $t = 4 \times 10^{-4}$ s, $n_r = n_z = n$

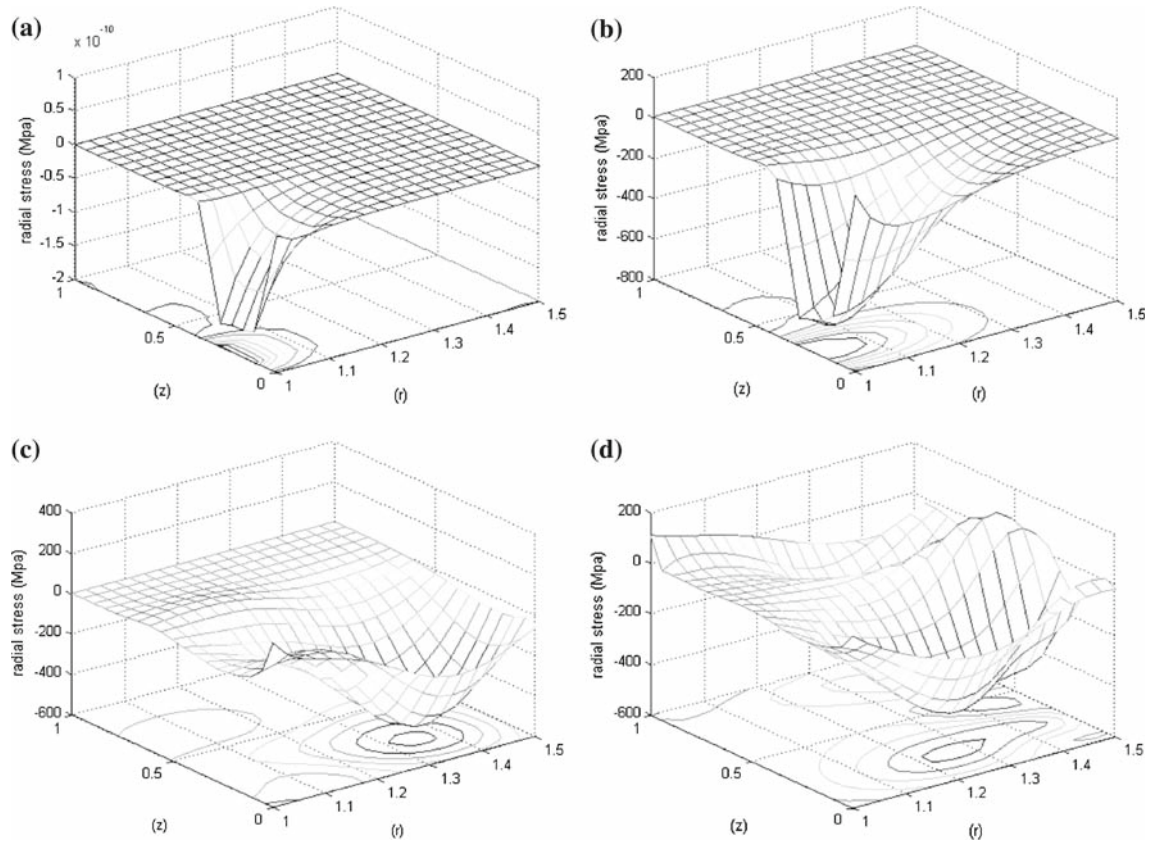


**Fig. 15** Radial stress distribution through the cylinder for $n_r = n_z = 0.5$ at **a** $t = 3\times10^{-5}$ s, **b** $t = 1.4\times10^{-4}$ s, **c** $t = 1.9\times10^{-4}$ s, **d** $t = 2.9 \times 10^{-4}$ s

cylinder cross-section at different times are shown. Powers of volume fraction distribution profiles are assumed as: $n_r = 0.5$ and $n_z = 0.5$.

The same results are plotted for different values of $n_r$ and $n_z$ in Figs. 16 and 17. The wave front for big values of "$n$" propagates faster than for small values of "$n$". The presented technique in this paper shows the acceptable method to calculate and analyze the dynamic behavior and wave propagation in 2D-FG structures. As it can be seen in Figs. 16 and 17, the radial stress wave propagation in the 2D domain is illustrated, and it is useful to calculate the peak point of the radial stress which is important in mechanical design.

It is clear from the results that stress wave propagation in two directions is strongly influenced by the material composition profile. In other words, the time response, the maximum amplitude and the uniformity of stress distribution through the cylinder can be modified to a required manner by selecting an appropriate material distribution profile. It is notable that the variation of the material distribution in two directions leads to a more flexible and desirable design which is very useful in optimization problems.

The manufacturing of multidimensional FGM may seem to be costly or difficult, but it should be noted that while these technologies are relatively new, processes such as 3D printing (3DP$^{TM}$) and Laser Engineering Net Shaping (LENS$^{(R)}$) can currently produce FGMs with relatively arbitrary tree-dimensional grading [25]. With further refinements FGM manufacturing methods may provide the designers with more control of the composition profile of functionally graded components with reasonable costs.

## 5 Conclusion

A 2D functionally graded cylinder with finite length under impact dynamic loading has been studied. For modeling and simulation of governing equations a graded finite element method is used which has some advantages to conventional finite element methods. The dynamic responses of a 2D-FGM cylinder are developed and the variations of different parameters with volume fraction exponents are obtained. The effects of

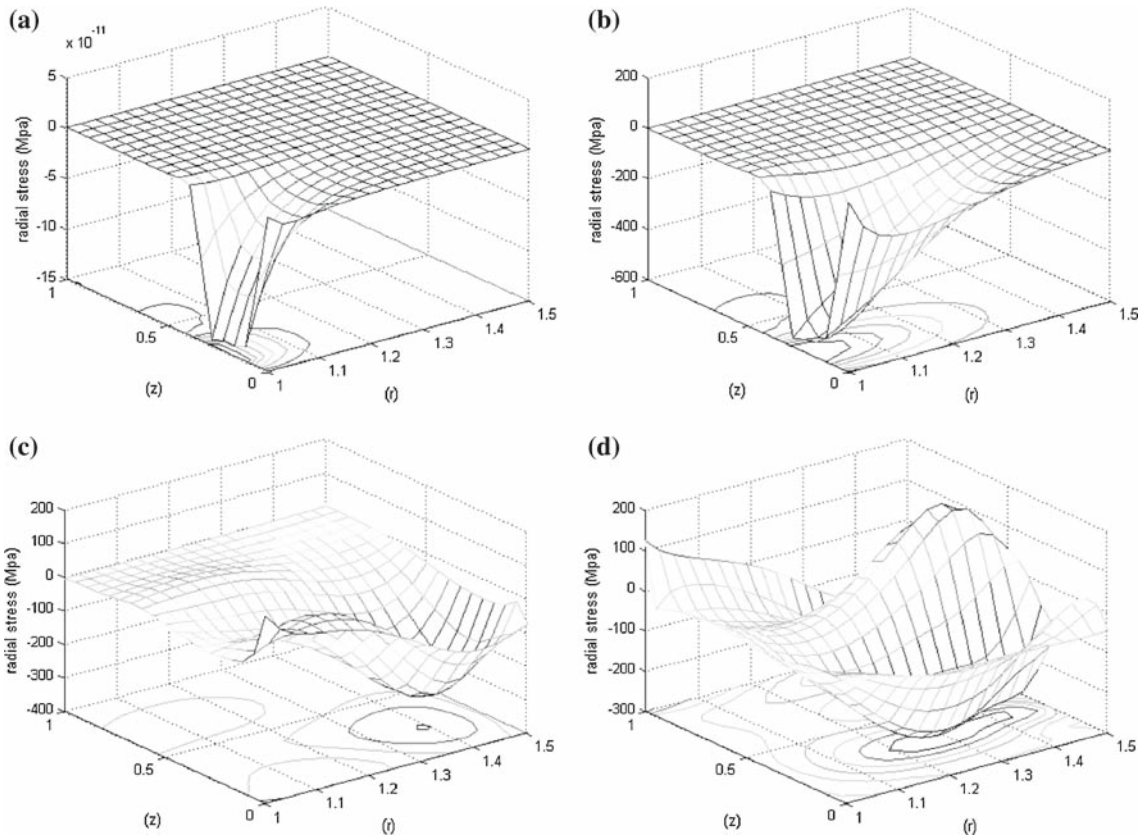


**Fig. 16** Radial stress distribution through the cylinder for $n_r = n_z = 1$ at **a** $t = 3 \times 10^{-5}$ s, **b** $t = 1.4 \times 10^{-4}$ s, **c** $t = 1.9 \times 10^{-4}$ s, **d** $t = 2.9 \times 10^{-4}$ s

2D material distribution on the wave propagation, stress distribution and time responses are considered and compared with conventional 1D-FGM. Based on the achieved results, 2D-FGMs have a powerful potential for designing and optimizing structures under multi-functional requirements. Time responses of the cylinder, maximum amplitude of stresses and uniformity of stress distribution can be modified to a required manner by selecting a suitable material distribution profile in two directions.

## Appendix

The matrix of linear interpolation functions is

$$[N] = \begin{bmatrix} N_i & 0 & N_j & 0 & N_k & 0 \\ 0 & N_i & 0 & N_j & 0 & N_k \end{bmatrix}, \tag{A.1}$$

where its components are

$$N_i = \frac{a_i + b_i r + c_i z}{2A}, \tag{A.2.1}$$

$$N_j = \frac{a_j + b_j r + c_j z}{2A}, \tag{A.2.2}$$

$$N_k = \frac{a_k + b_k r + c_k z}{2A}, \tag{A.2.3}$$

and

$$A = 1/2(r_i z_j + r_j z_k + r_i z_k - r_k z_j). \tag{A.3}$$

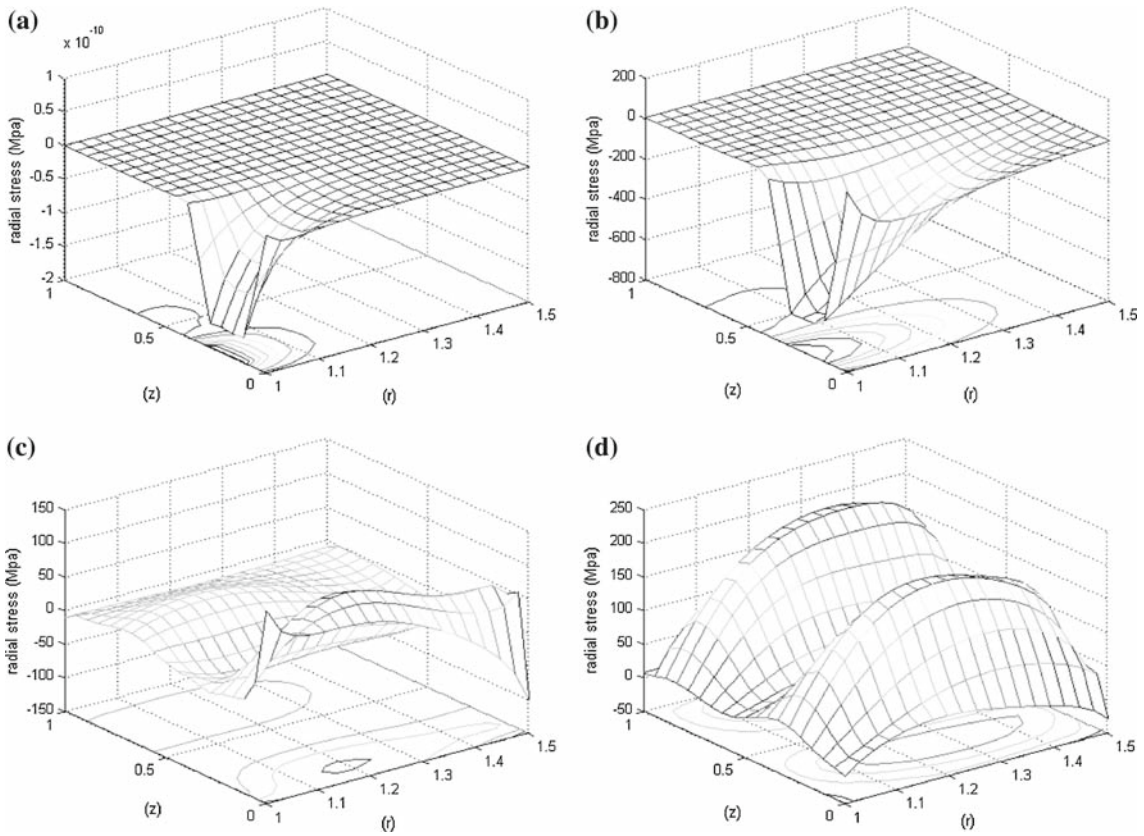


**Fig. 17** Radial stress distribution through the cylinder for $n_r = n_z = 5$ at **a** $t = 3 \times 10^{-5}$ s, **b** $t = 1.4 \times 10^{-4}$ s, **c** $t = 1.9 \times 10^{-4}$ s, **d** $t = 2.9 \times 10^{-4}$ s

The constants $a$, $b$ and $c$ are defined in terms of the nodal coordinates and $A$ is the area of the element,

$$\begin{aligned}
a_i &= r_j z_k - r_k z_j, \\
a_j &= r_i z_k - r_k z_i, \\
a_k &= r_i z_j - r_j z_i, \\
b_i &= z_j - z_k, \\
b_j &= z_k - z_i, \\
b_k &= z_i - z_j, \\
c_i &= r_j - r_k, \\
c_j &= r_k - r_i, \\
c_k &= r_i - r_j.
\end{aligned} \tag{A.4}$$

The vector of nodal displacements (degrees of freedom) is

$$\{Q^e\} = \begin{Bmatrix} u_i \\ w_i \\ u_j \\ w_j \\ u_k \\ w_k \end{Bmatrix}, \tag{A.5}$$

where subscripts $i$, $j$, $k$ are related to three nodes of each element. The vector of nodal forces for each element can be evaluated by the following integration:

$$\{F\}^e = \int\int_{s^e} [N]^{\mathrm{T}} \begin{Bmatrix} p_r \\ p_z \end{Bmatrix} \mathrm{d}s = \int_l \begin{bmatrix} N_i & 0 \\ 0 & N_i \\ N_j & 0 \\ 0 & N_j \\ N_k & 0 \\ 0 & N_k \end{bmatrix} \begin{Bmatrix} p_r \\ p_z \end{Bmatrix} 2\pi r \mathrm{d}l, \tag{A.6}$$

where $l$, $p_r$, $p_z$ denote the length of the edge under pressure, radial and axial components of pressure, respectively. In the present work $p_z = 0$ and $p_r = P_i(z, t)$ for each element.

The components of matrix $[B]$ are

$$B = \frac{1}{2A} \begin{bmatrix} b_i & 0 & b_j & 0 & b_k & 0 \\ N_i/r & 0 & N_j/r & 0 & N_k/r & 0 \\ 0 & c_i & 0 & c_j & 0 & c_k \\ c_i & b_i & c_j & b_j & c_k & b_k \end{bmatrix}. \tag{A.7}$$

## References


1. Koizumi, M.: The concept of FGM. Ceram. Trans. Funct. Graded Mater. **34**, 3–10 (1993)
2. Liu, G.R., Han, X., Lam K.Y.: Stress waves in functionally gradient materials and its use for material characterization. Compos. Part B Eng. **30**, 383–394 (1999)
3. Chiu, T.C., Erdogan, F.: One-dimensional wave propagation in a functionally graded elastic medium. J. Sound Vib. **222**, 453–487 (1999)
4. Bruck, H.A.: A one-dimensional model for designing functionally graded materials to manage stress waves. Int. J. Solids Struct. **37**, 6383–6395 (2000)
5. Li, Y., Ramesh, K.T., Chin, E.S.C.: Dynamic characterization of layered and graded structures under impulsive loading. Int. J. Solids Struct. **38**, 6045–6061 (2001)
6. Han, X., Liu, G.R., Lam, K.Y.: Transient waves in plates of functionally graded materials. Int. J. Numer. Methods Eng. **52**, 851–865 (2001)
7. Berezovski, A., Engelbrecht, J., Maugin, G.A.: Numerical simulation of two-dimensional wave propagation in functionally graded materials. Eur. J. Mech. A Solids **22**, 257–265 (2001)
8. Batra, R.C., Ching, H.K.: Analysis of elastodynamic deformations near a crack-notch tip by the meshless local Petrov–Galerkin (MLPG) method. Comput. Model. Eng. Sci. **3**, 717–730 (2002)
9. Zhang, G.M., Batra, R.C.: Wave propagation in functionally graded materials by modified smoothed particle hydrodynamics (MSPH) method. J. Comput. Phys. **222**, 374–390 (2007)
10. Shakeri, M., Akhlaghi, M., Hoseini, S.M.: Vibration and radial wave propagation velocity in functionally graded thick hollow cylinder. Compos. Struct. **76**, 174–181 (2006)
11. Hosseini, M., Akhlaghi, M., Shakeri, M.: Dynamic response and radial wave propagations of functionally graded thick hollow cylinder. Eng. Comput. **24**, 288–303 (2007)
12. Nemat-Alla, M.: Reduction of thermal stresses by developing twodimensional functionally graded materials. Int. J. Solids Struct. **40**, 7339–7356 (2003)
13. Dhaliwal, R.S., Singh, B.M.: On the theory of elasticity of a non-homogeneous medium. J. Elast. **8**, 211–219 (1978)
14. Clements, D.L., Budhi, W.S.: A boundary element method for the solution of a class of steady-state problems for anisotropic media. Heat Transf. **121**, 462–465 (1999)
15. Abudi, J., Pindera, M.J.: Thermoelastic theory for the response of materials functionally graded in two directions. Int. J. Solids Struct. **33**, 931–966 (1996)
16. Cho, J.R., Ha, D.Y.: Optimal tailoring of 2D volume-fraction distributions for heat-resisting functionally graded materials using FDM. Comput. Methods Appl. Mech. Eng. **191**, 3195–3211 (2002)
17. Hedia, H.S., Midany, T.T., Shabara, M.A.N., Fouda, N.: Development of cementless metal-backed acetabular cup prosthesis using functionally graded material. Int. J. Mech. Mater. Des. **2**, 259–267 (2005)
18. Santare, M.H., Thamburaj, P., Gazonas, A.: The use of graded finite elements in the study of elastic wave propagation in continuously non-homogeneous materials. Int. J. Solids Struct. **40**, 5621–5634 (2003)
19. Banks Sills, L., Eliasi, R., Berlin, Y.: Modeling of functionally graded materials in dynamic analyses. Compos. Part B. Eng. **33**, 7–15 (2002)
20. Scheidler, M.J., Gazonas, G.A.: Analytical and computational study of one-dimensional impact of graded elastic solids. In: Furnish, M.D. et al. (eds.) Shock Compression of Condensed Materials, pp. 689–692 (AIP CP620), Melville, NY, 2001. American Institute of Physics, Woodbury (2002)
21. Santare, M.H., Lambros, J.: Use of a graded finite element to model the behavior of nonhomogeneous materials. J. Appl. Mech. **67**, 819–822 (2000)
22. Kim, J.H., Paulino, G.H.: Isoparametric graded finite elements for nonhomogeneous isotropic and orthotropic materials. J. Appl. Mech. **69**, 502–514 (2002)

23. Zienkiewicz, O.C., Taylor, R.L.: The Finite Element Method, VII: Solid Mechanics, 5th edn. Butterworth-Heinemann, Oxford (2000)
24. Shao, Z.S.: Mechanical and thermal stresses of a functionally graded circular hollow cylinder with finite length. Int. J. Press. Vess. Pip. **82**, 155–163 (2005)
25. Goupee, A.J., Vel, S.S.: Two-dimensional optimization of material composition of functionally graded materials using meshless analyses and a genetic algorithm. Comput. Methods Appl. Mech. Eng. **195**, 5926–5948 (2006)